Measurement of Spin-Transfer Observables in $\bar{p}p \to \bar{\Lambda}\Lambda$ at 1.637 GeV/c

B. Bassalleck,[1] A. Berdoz,[2] C. Bradtke,[3] R. Bröders,[4] B. Bunker,[5] H. Dennert,[6] H. Dutz,[7] S. Eilerts,[1] W. Eyrich,[6] D. Fields,[1] H. Fischer,[8] G. Franklin,[2] J. Franz,[8] R. Gehring,[3] R. Geyer,[4] S. Goertz,[3] J. Harmsen,[3] J. Hauffe,[6] F. H. Heinsius,[8] D. Hertzog,[5] T. Johansson,[9] T. Jones,[5] P. Khaustov,[2] K. Kilian,[4] P. Kingsberry,[1] E. Kriegler,[8] J. Lowe,[1] A. Meier,[3] A. Metzger,[6] C. A. Meyer,[2] W. Meyer,[3] M. Moosburger,[6] W. Oelert,[4] K. D. Paschke,[2,*] M. Plückthun,[7] S. Pomp,[9] B. Quinn,[2] E. Radtke,[3] G. Reicherz,[3] K. Röhrich,[4,†] K. Sachs,[4] H. Schmitt,[8] B. Schoch,[7] T. Sefzick,[4] F. Stinzing,[6] R. Stotzer,[1] R. Tayloe,[5,‡] and St. Wirth[6]

(PS185 Collaboration)

[1]*University of New Mexico, Albuquerque, New Mexico 87131*
[2]*Carnegie Mellon University, Pittsburgh, Pennsylvania 15213*
[3]*Ruhr-Universität Bochum, D-44780 Bochum, Germany*
[4]*Institut für Kernphysik des Forschungszentrums Jülich, D-52425 Jülich, Germany*
[5]*University of Illinois, Urbana, Illinois 61801*
[6]*Universität Erlangen-Nürnberg, D-91058 Erlangen, Germany*
[7]*Universität Bonn, D-53115 Bonn, Germany*
[8]*Universität Freiburg, D-79104 Freiburg, Germany*
[9]*Uppsala University, S-75121 Uppsala, Sweden*
(Received 2 June 2002; published 31 October 2002)

Spin-transfer observables for $\bar{p}p \to \bar{\Lambda}\Lambda$ have been measured using a transversely polarized frozen-spin target and a beam momentum of 1.637 GeV/c. Current models of the reaction near threshold are in good agreement with existing measurements performed with unpolarized particles in the initial state but produce conflicting predictions for the spin-transfer observables D_{nn} and K_{nn} (the normal-to-normal depolarization and polarization transfer), which are measurable only with polarized target or beam. Measurements of D_{nn} and K_{nn} presented here are found to be in disagreement with predictions from these models.

The measurement of near-threshold exclusive antihyperon-hyperon ($\bar{Y}Y$) production in antiproton-proton reactions has proven to be a powerful tool in the study of the dynamics of the $\bar{q}q$ annihilation and production mechanisms. These reactions have been extensively studied by the PS185 Collaboration at the Low Energy Antiproton Ring (LEAR) facility at CERN, which has produced the overwhelming majority of the existing data on exclusive $\bar{p}p \to \bar{Y}Y$ near threshold, including cross-sections and final-state polarization and spin correlations [1,2]. In particular, high-precision measurements have been made of $\bar{\Lambda}\Lambda$ production over a kinematic range from very near threshold to about 200 MeV of excess energy in the center-of-mass system.

The features of the $\bar{p}p \to \bar{\Lambda}\Lambda$ reaction have been reproduced by various models which describe the reaction dynamics either in a meson-exchange framework [3–6] or with a QCD-inspired effective theory [7–9]. In the meson-exchange model (MEX), the transition occurs through the t-channel exchange of a strange meson, with the $K(494)$ and $K^*(892)$ most often found to provide the most significant contributions [5,6]. The QCD-inspired "quark-gluon" (QG) model is an effective theory describing an s-channel exchange with well-

defined quantum numbers corresponding to specific QCD degrees of freedom, such as $^3S_1$ (single-gluon exchange) or $^3P_0$ (multiple-gluon exchange with the quantum numbers of the vacuum) [7–9]. In both formulations, the initial-state and final-state interactions contribute significantly to the features of the reaction. Although the initial-state interactions (ISI) are constrained by $\bar{p}p$ elastic and inelastic scattering data, no similar data exist to constrain the $\bar{\Lambda}\Lambda$ final-state interaction (FSI).

Given the uncertainty in initial- and final-state interactions, as well as freedom in adjusting coupling strengths, calculations based on each of these two approaches have successfully reproduced the previously measured observables, although these calculations are quite different in predictions of the reaction dynamics [5,6,9]. One prominent disagreement between the models is the role of the tensor interaction. MEX calculations lead to a dominant tensor force resulting from a constructive interference of the K and K^* in the tensor channel. This tensor interaction couples only to triplet ($S = 1$) final states and serves to explain the near absence of singlet-state production seen in earlier measurements [1,2]. The QG approach, which includes only couplings

to triplet-state quantum numbers, incorporates complete triplet dominance by construction while finding only a relatively small tensor interaction, even when fully accounting for the ISI and FSI.

In the measurement described here, the role of the tensor interaction in $\bar{p}p \rightarrow \bar{\Lambda}\Lambda$ is probed through measurements of the spin-transfer observables, which describe correlations between the initial- and final-state polarizations. The depolarization D_{nn} measures spin transfer from the target proton's component normal to the scattering plane to the normal component for the produced Λ and is defined such that

$$\langle \vec{\boldsymbol{\sigma}}_{\Lambda} \cdot \hat{\boldsymbol{n}} \rangle = \frac{P_n + D_{nn}\vec{\boldsymbol{P}}_T \cdot \hat{\boldsymbol{n}}}{1 + A_n \vec{\boldsymbol{P}}_T \cdot \hat{\boldsymbol{n}}}. \qquad (1)$$

The polarization transfer K_{nn} analogously measures the normal-to-normal transfer of spin from the target proton to the produced $\bar{\Lambda}$:

$$\langle \vec{\boldsymbol{\sigma}}_{\bar{\Lambda}} \cdot \hat{\boldsymbol{n}} \rangle = \frac{P_n + K_{nn}\vec{\boldsymbol{P}}_T \cdot \hat{\boldsymbol{n}}}{1 + A_n \vec{\boldsymbol{P}}_T \cdot \hat{\boldsymbol{n}}}. \qquad (2)$$

In these expressions, $\langle \vec{\boldsymbol{\sigma}} \cdot \hat{\boldsymbol{n}} \rangle$ is twice the average value of the spin component along the normal to the scattering plane, $\hat{\boldsymbol{n}}$. The direction of $\hat{\boldsymbol{n}}$ is defined in terms of the incident and outgoing particle momenta, with $\hat{\boldsymbol{n}}$ in the direction of $\vec{\boldsymbol{p}}_{\bar{p}} \times \vec{\boldsymbol{p}}_{\bar{\Lambda}}$. Also, $\vec{\boldsymbol{P}}_T$ is the target proton polarization, P_n is the polarization of the Λ and $\bar{\Lambda}$ in the $\hat{\boldsymbol{n}}$ direction for production with no initial-state polarization, and A_n is the left-right asymmetry of $\bar{\Lambda}\Lambda$ production with a polarized target.

Since the tensor interaction prefers spin-flip transitions between the initial and final states, the MEX calculations predict a strongly negative D_{nn} and K_{nn}. In contrast, the QG calculations include only a minor tensor component and consequently predict less spin flip and positive values for D_{nn} and K_{nn}. This difference in the predictions of the models has been shown to be largely insensitive to inclusion of the ISI and FSI [6,9].

Previous PS185 results on spin observables have been limited to final-state spins, which could be determined from event topology distributions since the self-analyzing weak decay of the hyperon correlates the direction of the decay products with the hyperon spin. The measurement of spin-transfer observables requires the use of a polarized target or beam. The experiment described in this Letter used a frozen-spin target and represents the first measurement of such observables for exclusive $\bar{Y}Y$ production from $\bar{p}p$ annihilation in the near-threshold region [10]. It provides a stringent, new test for models which have successfully reproduced previous measurements of this reaction.

The detector system, which was essentially the same as that used for previous PS185 measurements, has been described in several publications [1]. The products of

the charged decay of the hyperons were tracked in 10 planes of multiwire proportional chamber followed by 13 planes of drift chamber. The topology of these four tracks, along with the well-known masses of the nucleons, hyperons, and pions, overdetermines the kinematics of each event. A fit of the kinematics of the reaction to this topology provides a precise measurement of the center-of-mass production and decay angles, as well as a clear method for distinguishing the signal events from background through the fit quality. There were no magnetic fields in these tracking chambers, leaving an ambiguity between the $\bar{\Lambda}$ and Λ. This ambiguity was resolved by using three additional drift planes to detect the horizontal deflection of each track in a vertical magnetic field contained in a solenoid behind the tracking chambers.

The trigger system, which took advantage of the charged-neutral-charged signature of the event topology, was also similar to that used in previous PS185 measurements, although it required modification to accommodate the frozen-spin target. The trigger was initiated by scintillators upstream of the target, which detected the incident $\bar{p}$. The trigger was vetoed by scintillators downstream and to the sides of the target, thus requiring neutral particles exiting the target, consistent with $\bar{\Lambda}\Lambda$ production. The trigger was completed by coincidence with hits in a scintillator hodoscope positioned downstream of the tracking chambers, which indicated the passage of charged tracks through the active detector volume as expected for the charged decay of the hyperons.

A transversely polarized frozen-spin target [11,12] was used to provide access to the spin-transfer observables. This target was a 6 mm diameter, 9 mm long cylinder of butanol submerged in a liquid He bath, with the cylindrical axis along the beam direction. The cryostat, which incorporated a superconducting solenoid to produce the holding field, was a vertical cylinder with an outer diameter of only 42 mm. This small cryostat size allowed the trigger-veto scintillators to be positioned close to the production target. The close positioning of these scintillators was critical to maintain trigger efficiency, as any hyperon which decayed upstream of them caused the event to be vetoed. The polarization of the target was determined using NMR measurements to fix the initial and final points of the relaxation curve for each data-taking period [13]. The magnitude of target polarization averaged 62% during data production.

A detailed, GEANT-based Monte Carlo simulation [14] of the detection and analysis procedures was used to study the effects of imperfect geometric acceptance and reconstruction efficiency. The detection-efficiency correction was large, due primarily to the stringent trigger requirements. Over 80% of the $\bar{\Lambda}\Lambda$ events that underwent doubly charged decay were rejected because of a decay upstream of the veto. The effects of this trigger

inefficiency were accurately reproduced by the detector simulation, as confirmed by the extraction of proper lifetime distributions. This simulation also included the effects of multiple Coulomb scattering of charged particles and hadronic interactions in the target and detector regions, which significantly affected the event reconstruction efficiency.

The target polarization sign was flipped during data collection, so that approximately half of the total integrated luminosity was collected in each target polarization state in order to control possible sources of systematic error. A total of 1.2×10^{11} antiprotons were observed incident on the 9 mm thick target, producing 30 818 events which exhibited topology which could be cleanly fit by the kinematic hypothesis of $\bar{\Lambda}\Lambda$ production from a free proton and subsequent doubly charged decay. These events were sorted into 16 bins of variable size over $\cos\theta_{c.m.}$. The sizes of the bins were adjusted to approximately match the statistics between them.

The results presented in this Letter, for the observables D_{nn}, K_{nn}, and the singlet fraction S_F as a function of the center-of-mass scattering angle $\cos\theta_{c.m.}$, were extracted, simultaneously with other observables, through the use of the spin-scattering matrix formalism. Sensitivity to the parameters of the scattering matrix, which has recently been demonstrated [15], depends on transverse polarization of at least one initial-state particle as well as the self-analyzing property of the hyperon weak decay. The statistical error estimates for these results were determined by finding the limits of contours on the multidimensional log-likelihood function surface [16]. Because of correlations in parameter space, these error estimates are significantly asymmetric for some observables in some bins of $\cos\theta_{c.m.}$. Details of the extraction of scattering-matrix parameters and the uncertainty analysis, along with results for a larger set of observables, will be presented in a future publication. For those observables which could also be extracted from previous measurements performed without target polarization, good agreement is found between the published results [2] and the corresponding observables found from this fit of the complete set of parameters of the spin-scattering matrix.

Figure 1 shows results for the depolarization D_{nn} and polarization transfer K_{nn}, along with predictions from full QG [9] and MEX [6] calculations which include ISI and FSI effects. These results clearly indicate a failure of both models to correctly describe the reaction dynamics in this kinematic region.

In the backward scattering region, D_{nn} remains near zero, indicating that the target proton and Λ spin are uncorrelated along the scattering plane normal. This contrasts with K_{nn}, which grows from near zero at $\cos\theta_{c.m.}$ to an average value of ~ 0.75 for $\cos\theta_{c.m.} < -0.75$, indicating a strong, positive correlation between the target proton spin and the spin of the $\bar{\Lambda}$. The positive correlation
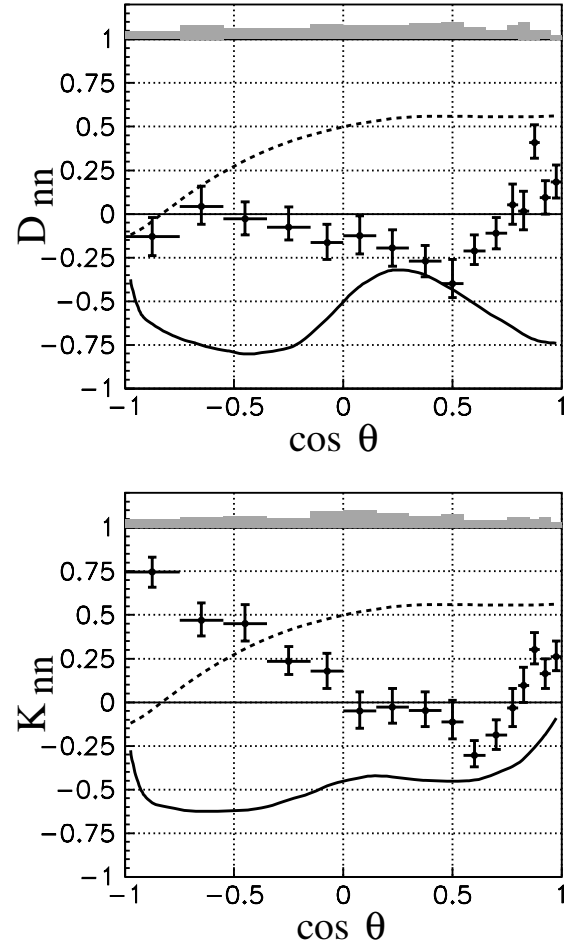

FIG. 1. Results for D_{nn} and K_{nn} for $\bar{p}p \to \bar{\Lambda}\Lambda$ at 1.637 GeV/c. The error bars indicate 1σ statistical uncertainty estimates and are asymmetric for some data points. The systematic uncertainty estimates are shown by the shaded boxes at the top of the figure. Predictions from the QG model [9] (dotted line) and the MEX model [6] (solid line) are superimposed.

between the initial-state baryon and the final-state antibaryon in this range of $\cos\theta_{c.m.}$ was not predicted by either the MEX or the QG models.

It is straightforward to demonstrate, using the spin-scattering matrix formalism, that D_{nn} and K_{nn} are restricted to be equal in the case of pure triplet-state production of the $\bar{\Lambda}\Lambda$ final state [17]. Therefore, the observed deviation between D_{nn} and K_{nn} serves to emphasize the significance of the small but nonzero singlet contribution in the final state. The relative strength of the singlet and triplet components defines the singlet fraction observable, S_F, such that

$$\langle \vec{\boldsymbol{\sigma}}_{\bar{\Lambda}} \cdot \vec{\boldsymbol{\sigma}}_{\Lambda} \rangle = \frac{1 + 4S_F}{1 + A_n \vec{\boldsymbol{P}}_T \cdot \hat{\boldsymbol{n}}}. \qquad (3)$$

$S_F = 1$ would signify pure singlet-state production while $S_F = 0$ would imply pure triplet-state production. This observable has been measured, by previous

PS185 studies performed with an unpolarized target, to be near zero in the near-threshold kinematic region. Measurements for S_F have often been quoted as an average over center-of-mass production angle $\cos\theta_{\text{c.m.}}$, in which the strongly forward-peaked cross section weights the singlet-dominated forward-angle production more heavily. Results for this observable from the current analysis as a function of $\cos\theta_{\text{c.m.}}$ are shown in Fig. 2, along with results from a previous measurement at similar kinematics. There is good agreement between results from the two measurements, which indicate that S_F is very near zero for production in the forward direction and is small, but nonzero, for back-angle production.

This behavior is not well described by either the MEX or the QG model. Without a small but significantly non-zero singlet-state component in the back-angle production, no description of the production dynamics will be able to accommodate the observed deviation between D_{nn} and K_{nn}. In the case of the QG model, only triplet-state transitions are allowed so the model, by construction, describes a vanishing singlet fraction for all values of $\cos\theta_{\text{c.m.}}$. It is possible that the QG description could be improved with the inclusion of some singlet-state coupling, such as the pseudoscalar $^1S_0$ transition, although previous studies have concluded that this transition was insignificant [18]. While the MEX description is not so extreme with regard to the singlet contribution, it also does not correctly describe the rising back-angle singlet fraction and so fails to predict the deviation between D_{nn} and K_{nn}. In principle, these models can accommodate an increased singlet contribution. Even with a somewhat reduced triplet-state strength, the MEX approach would tend to predict a dominant spin flip between the initial and final states, which has been clearly excluded by the current measurements.

There has been some recent theoretical speculation about the connection between the near-threshold $\bar{Y}Y$ production studies and the nonvalence quark contributions to the nucleon spin [19,20]. Mechanisms for describing $\bar{p}p \to \bar{\Lambda}\Lambda$ have been discussed which involve preexisting polarized strange quarks or polarized glue in the nucleon wave function. Although no quantitative predictions have been made for D_{nn} or K_{nn} with these models, the results presented here are not consistent with the qualitative predictions from either of these alternative production mechanisms alone [19].

In addition to the observables presented here, numerous other observables have been extracted, as has the full set of parameters of the spin-scattering matrix [21], which will be shown in a future publication. The breadth of these results presents an opportunity for the further development of models describing the dynamics of the $\bar{p}p \to \bar{\Lambda}\Lambda$ reaction.
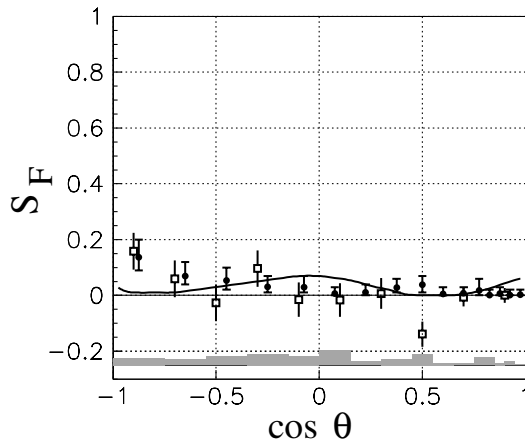
FIG. 2.   Current results for the singlet fraction S_F for $\bar{p}p \to \bar{\Lambda}\Lambda$ at $1.637\,\text{GeV}/c$ (solid circles) shown with asymmetric statistical error bars, superimposed with results from a previous measurement performed with an unpolarized target at $1.642\,\text{GeV}/c$ (hollow squares) [2] shown with symmetric statistical error bars. The systematic uncertainty estimate for the current measurement is shown by the shaded boxes at the bottom of the figure. Predictions from the MEX model [6] (solid line) are superimposed. The QG model predicts $S_F = 0$ uniformly [9].

*Present address: University of Massachusetts, Amherst, MA 01003.
Electronic address: paschke@jlab.org
†Present address: Creative Services, F-01630 Saint Genis-Pouilly, France.
‡Present address: University of Indiana, Bloomington, IN 47408.

[1] PS185 Collaboration, P. D. Barnes *et al.*, Phys. Lett. B **189**, 249 (1987); PS185 Collaboration, P. D. Barnes *et al.*, Phys. Lett. B **199**, 147 (1987); PS185 Collaboration, P. D. Barnes *et al.*, Phys. Lett. B **229**, 432 (1989); PS185 Collaboration, P. D. Barnes *et al.*, Phys. Lett. B **246**, 273 (1990); PS185 Collaboration, P. D. Barnes *et al.*, Nucl. Phys. **A526**, 575 (1991); PS185 Collaboration, P. D. Barnes *et al.*, Phys. Lett. B **309**, 469 (1993); PS185 Collaboration, P. D. Barnes *et al.*, Phys. Lett. B **331**, 203 (1994); PS185 Collaboration, P. D. Barnes *et al.*, Phys. Rev. C **54**, 1877 (1996); PS185 Collaboration, P. D. Barnes *et al.*, Nucl. Phys. B (Proc. Suppl.) **56A**, 46 (1997).
[2] PS185 Collaboration, P. D. Barnes *et al.*, Phys. Rev. C **54**, 2831 (1996).
[3] F. Tabakin and R. A. Eisenstein, Phys. Rev. C **31**, 1857 (1985).

[4] P. LaFrance and B. Loiseau, Nucl. Phys. **A528**, 557 (1991).

[5] R. G. E. Timmermans, Th. A. Rijken, and J. J. de Swart, Phys. Rev. D **45**, 2288 (1992).

[6] J. Haidenbauer, K. Holinde, V. Mull, and J. Speth, Phys. Lett. B **291**, 223 (1992); Phys. Rev. C **46**, 2158 (1992).

[7] S. Furui and A. Faessler, Nucl. Phys. **A468**, 669 (1987).

[8] M. Kohno and W. Weise, Phys. Lett. B **206**, 584 (1988).

[9] M. A. Alberg, E. M. Henley, P. D. Kunz, and L. Wilets, Nucl. Phys. **A560**, 365 (1993); Phys. At. Nucl. **57**, 1608 (1994).

[10] PS185 Collaboration, B. Bassalleck *et al.*, CERN Report No. CERN/SPSLC-95-13/P287, 1995.

[11] H. Dutz *et al.*, Nucl. Instrum. Methods Phys. Res., Sect. A **A340**, 272 (1994).

[12] M. Plückthun, Ph.D. thesis, Universität Bonn, 1998 (Universität Bonn Report No. BONN-IR-98-04).

[13] M. Plückthun *et al.*, Nucl. Instrum. Methods Phys. Res., Sect. A **400**, 133 (1997).

[14] Applications Software Group, Computing and Networks Division, GEANT: *Detector Description and Simulation Tool* (CERN, Geneva, 1993).

[15] K. D. Paschke and B. Quinn, Phys. Lett. B **495**, 49 (2000).

[16] W. T. Eadie, D. Drijard, F. E. James, M. Roos, and B. Sadoulet, *Statistical Methods in Experimental Physics* (North-Holland Publishing Company, Amsterdam, 1971).

[17] M. Elchikh and J.-M. Richard, Phys. Rev. C **61**, 035205 (2000).

[18] M. Alberg, E. M. Henley, and W. Weise, Phys. Lett. B **255**, 498 (1991).

[19] M. Alberg, J. Ellis, and D. Kharzeev, Phys. Lett. B **356**, 113 (1995).

[20] J. Ellis, M. Karliner, D. E. Kharzeev, and M. G. Sapozhnikov, Nucl. Phys. **A673**, 256 (2000).

[21] K. Paschke, Ph.D. thesis, Carnegie Mellon University, 2001.